Evidence of Two Viscous Relaxation Processes in the Collective Dynamics of Liquid Lithium

T. Scopigno,[1] U. Balucani,[2] G. Ruocco,[3] and F. Sette[4]
[1]*Dipartimento di Fisica and INFM, Universitá di Trento, I-38100, Povo, Italy*
[2]*Istituto di Elettronica Quantistica CNR, I-50127, Firenze, Italy*
[3]*Dipartimento di Fisica and INFM, Universitá di L'Aquila, I-67100, L'Aquila, Italy*
[4]*European Synchrotron Radiation Facility, B.P. 220, F-38043 Grenoble, Cedex France*
(Received 14 March 2000)

New inelastic x-ray scattering experiments have been performed on liquid lithium in a wide wave vector range. With respect to the previous measurements, the instrumental resolution, improved up to 1.5 meV, allows one to accurately investigate the dynamical processes determining the observed shape of the dynamic structure factor $S(Q, \omega)$. A detailed analysis of the line shapes shows the coexistence of relaxation processes with both slow and fast characteristic time scales, and therefore shows that pictures of the relaxation mechanisms based on a simple viscoelastic model must be abandoned.

PACS numbers: 61.25.Mv, 61.20.Lc, 67.40.Fd

The collective dynamics of liquid alkali metals exhibits several features which make these systems excellent candidates to test different theories on the microdynamics of the liquid state. In simple liquids, both generalized kinetic theory and mode-coupling treatments predict the existence of two distinct relaxation processes affecting the dynamics of density fluctuations [1]. In these theories the dominant damping mechanism is provided by a fast process which is thought to be associated with the interactions between an atom and the "cage" of its nearest neighbors. In addition, one should also detect a much slower process involving the cooperative motion of a larger number of particles, which rearranges the local structure to ultimately restore equilibrium, and which is responsible for the critical slowing down in those systems capable of supercooling. In simple liquids such as the molten alkali metals most of these predictions have been tested by molecular dynamics (MD) simulations [2]. In these numerical studies several phenomena have been detected, such as the persistence of well-defined density modes outside the strict hydrodynamic region and an increase of the sound velocity in the mesoscopic wave vector region (the so-called "positive dispersion"). More recently, considerable attention has been devoted to checking the existence of the afore-mentioned relaxation mechanisms [3,4].

Up to few years ago, the only experimental technique capable of accessing the relevant wavevector/frequency range was inelastic neutron scattering (INS). Studies were reported on rubidium [5], cesium [6], lithium [7,8], potassium [9] and again rubidium [10]. Probing wave vectors Q up to the first sharp diffraction peak, collective excitations outside the strict hydrodynamic regime were detected. The INS data have usually been analyzed with very simple models and, in the favorable cases (scattering cross section mostly coherent and speed of sound low enough to overcome kinematics restrictions), it was possible to observe the positive dispersion of the sound velocity of the acoustic mode—one of the features predicted by the MD simulations. This situation is exemplified by the INS experiments of Bodensteiner *et al.* in liquid cesium [6], where the quality of the data allowed even testing of the line shape predicted by the viscoelastic model, a sort of simplified relaxation mechanism with a single (average) decay time. However, even in this case, the data accuracy did not allow one to test whether the two (physically quite different) mechanisms mentioned previously appear in the experimental determination of the $S(Q, \omega)$.

The development of inelastic x-ray scattering (IXS) technique paved the way for the experimental investigations of the collective dynamics of liquids in the mesoscopic region. The aim of the present work is to report very high quality IXS data of the $S(Q, \omega)$ of liquid lithium, a case particularly unfavorable to INS but showing remarkable inelastic features [11]. These data allow one to accurately study the spectral shape, and to obtain the first strong evidence on the existence of a double-time-scale decay mechanism underlying the dynamics of density fluctuations. The adoption of a spectral analysis scheme based on the generalized Langevin equation formalism, enables us to extract quantitative information on the relaxation processes.

The IXS experiment was carried out at the high resolution beam line ID16 of the European Synchrotron Radiation Facility (Grenoble, F). The backscattering monochromator and analyzer crystals, operating at the (hhh) silicon reflections with $h = 9, 11$, gave a total energy resolution of 3 meV for $h = 9$ and 1.5 meV for $h = 11$. The wave vector transferred in the scattering process was selected between 1.4 and 25 nm^{-1} by rotating a 7 m long analyzer arm in the horizontal scattering plane. The total Q resolution was set to 0.4 nm^{-1}. Energy scans, performed by varying the temperature of the monochromator with respect to that of the analyzer crystals, took about 180 min, and each spectrum at a given Q was obtained from the average of 2 to 8 scans, depending on the values of h and of Q. The sample (Goodfellows) had a nominal purity better than 0.001. The liquid lithium uncapped container was made of austenitic stainless steel,

 0031-9007/00/85(19)/4076(4)$15.00

and a resistance heater was used to keep the liquid at 475 K, i.e., slightly above the melting point at 453 K. Additional data were collected at 600 K. The 20 mm long sample, kept together by surface tension, was maintained in a 10^{-6} mbar vacuum and loaded in an argon glove box. In the $Q - E$ region of interest, empty vacuum chamber measurements gave either the flat electronic detector background of 0.6 counts/min ($Q > 8$ nm^{-1}), or, for $Q < 8$ nm^{-1} a small elastic line due to scattering from the chamber kapton windows (each 50 μm thick). This signal, after proper normalization, has been subtracted from the raw data. The scattered intensity $I(Q, \omega)$ was reduced to absolute units following a procedure described in Ref. [12], and the contribution from multiple scattering was negligible [13].

Typical spectra are reported in Fig. 1 (open circles).

The data analysis has been performed starting from a generalized Langevin equation:

$$\ddot{\phi}(Q,t) + \omega_0^2(Q)\phi(Q,t) + \int_0^t M(Q,t-t')\dot{\phi}(Q,t')\,dt' = 0\,,$$

[here $\omega_0^2(Q) = [k_B T/mS(Q)]Q^2$] obtained adopting a standard memory function approach for the density correlator $\phi(Q,t) = \langle \rho_Q(t)\rho_{-Q}(0)\rangle/\langle|\rho_Q(t)|^2\rangle$ where $\rho(t) = (1/N)\sum_i e^{-i\mathbf{Q}\cdot\mathbf{r}_i(t)}$, and $\langle|\rho_Q(t)|^2\rangle = S(Q)$, the static structure factor. After solving this equation, the dynamic structure factor reads [1,15] as

$$\frac{S(Q,\omega)}{S(Q)} = \frac{\pi^{-1}\omega_0^2(Q)M'(Q,\omega)}{[\omega^2 - \omega_0^2 + \omega M''(Q,\omega)]^2 + [\omega M'(Q,\omega)]^2}\,. \tag{1}$$

In Eq. (1), all the details of the microscopic interactions are embodied in the (complex) "memory function" $M(Q,t)$, which is conveniently written as a sum of a longitudinal "viscous" contribution $M_L(Q,t)$ and of a term $M_{\rm th}(Q,t)$ arising from the coupling to thermal fluctuations. In the $Q \to 0$ hydrodynamic regime, the memory function $M(Q,t) = M_L(Q,t) + M_{\rm th}(Q,t)$ can be written as

$$\begin{aligned} M(Q,t) &= M_L(Q,t) + M_{\rm th}(Q,t) \\ &= 2(\eta_L/nm)Q^2\delta(t) + (\gamma - 1)\omega_0^2(Q)e^{-D_T Q^2 t}, \end{aligned} \tag{2}$$

where η_L is the longitudinal viscosity, n the number density, γ the specific heat ratio, and D_T the thermal diffusivity. In the case of liquid metals, the inaccuracy of the expression (2) at finite wave vectors is particularly evident: due to the large thermal diffusivity of these systems, the second term in Eq. (2) is in fact instantaneous, and the line shape deduced from Eq. (1) is the so called "damped oscillator model" (DHO). This scheme is unable to account for the quasielastic peaks evident from the spectra in Fig. 1, and thus must be discarded (for further details, see Ref. [12]). A reasonable way to improve the simple hydrodynamic, DHO-like, model (2) is to allow a noninstantaneous decay of the viscous term $M_L(Q,t)$. On a practical basis, the simplest way of doing this is to assume multiple exponential decay laws for the time dependence of $M_L(Q,t)$:

$$M_L(Q,t) = \Sigma_{i=1}^N \Delta_i^2(Q)e^{-t/\tau_i(Q)}, \tag{3}$$

and to perform a refined analysis of the data by increasing N until optimum agreement is obtained. In a first step, we have taken $N = 1$, which corresponds to the usual viscoelastic model. Then we tested the case $N = 2$, which mimics the two time scales' theoretical predictions, an ansatz for $M_L(Q,t)$ that was proposed to account for the details of $S(Q,\omega)$ in the MD simulations of Lennard-Jones liquids [16]. Despite its arbitrary character, the exponential decay law in Eq. (3) has the advantage of yielding analytical Fourier transforms, thereby simplifying considerably the fitting procedure.

The scattered intensity is proportional to the convolution between the experimental resolution function $R(\omega)$ and a "quantum-mechanical" dynamic structure factor $S_q(Q,\omega)$, affected by the detailed balance condition:

$$S_q(Q,\omega) = \beta\hbar\omega/(1 - e^{-\beta\hbar\omega})S(Q,\omega)\,. \tag{4}$$

The difference between the resulting function and the experimental data has been minimized using a Levenberg-Marquardt procedure. $\omega_0^2(Q)$ has been obtained from its definition, while the quantities γ and D_T have been fixed to their experimental $Q \to 0$ values, the latter being taken from Ref. [17]. Consequently, the only free parameters in the fitting iterations were the decay times $\tau_i(Q)$, and the strengths of the viscous relaxations $\Delta_i^2(Q)$. As a result, we have been able to fit our data all over the explored Q range, and to find striking differences between the use of one or two relaxation mechanisms. The results (resolution convoluted) are shown in Fig. 1 for the data taken at the three reported Q values. The dashed/dotted and solid lines correspond, respectively, to the fit with one or two exponential functions. The fitting results provide definite evidence that the one decay-time viscoelastic model is untenable. On the contrary, a two time scale relaxation dynamics for the decay of $M_L(Q,t)$ successfully accounts for the observed spectral shapes yielding an excellent fit (full line). The single-time viscoelastic fits [$N = 1$ in Eq. (3)], both initialized with free parameters corresponding to the best values obtained in the two-times model, give results that can be read as a sort of "average" of the two processes, emphasizing in turn either the fast or the slow one. From this comparison one notices that the faster relaxation process accounts almost entirely for the width of the inelastic peak and for the broader part of the quasielastic region, while the slower relaxation is responsible for the narrow portion of the central peak.

Following the theoretical analysis of Ref. [18], we shall refer to the faster mechanism as "microscopic" (label μ)

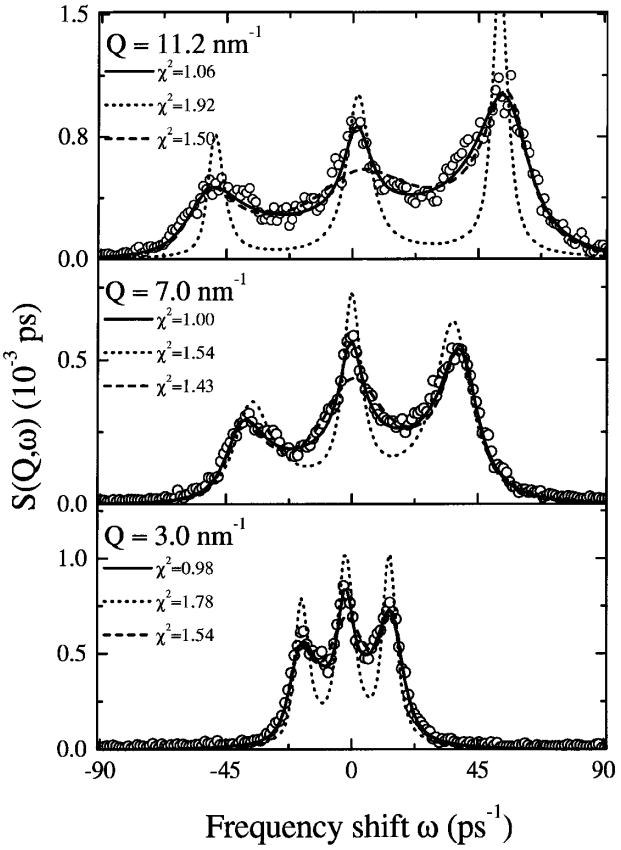

FIG. 1. IXS spectra of liquid lithium at $T = 475$ K at three wave vectors. Open circles: experimental data. Dashed/dotted lines: results of two fitting sessions (resolution convoluted) with comparable χ^2 for a memory function model which includes thermal decay and a single-time viscous relaxation channel (viscoelastic model). Full line: same as before, except that now the viscous relaxation proceeds with two decay channels (microscopic and structural relaxation). Normalized χ^2 values are also reported, the expected value is 1 ± 0.1.

and to the slower one as "structural" (label α). In Fig. 2 we report for the investigated temperatures the ratio $A(Q)$ between the strengths of the slow process $\Delta^2_\alpha(Q)$ and the total strength $\Delta^2_\alpha(Q) + \Delta^2_\mu(Q)$ as found from the fitting procedure. The weight of the structural mechanism is seen to be largest at the smallest wave vectors ($\sim$20%), and to decrease with Q. This is in agreement with the expectation that the slower relaxation process affects less the dynamics of the systems as one increases the frequency to values sensibly larger than $1/\tau_\alpha$.

The wave vector dependence of the relaxation times is illustrated in Fig. 3. The microscopic time turns out to be nearly temperature independent, with values of $\tau_\mu(Q)$ decreasing in the explored Q range from $\sim$0.05 ps down to $\sim$0.01 ps. The values of the relaxation time $\tau_\alpha(Q)$ associated with the structural process are instead more scattered: $\tau_\alpha(Q)$ is always of the same order as the inverse of the energy resolution [$\sim$0.43 ps in the case of the (9 9 9) reflection], making rather difficult a precise determination.

Finally, in Fig. 4 we report the Q dependence of the sound speed $c_l(Q) = \omega_l(Q)/Q$ where $\omega_l(Q)$ is the

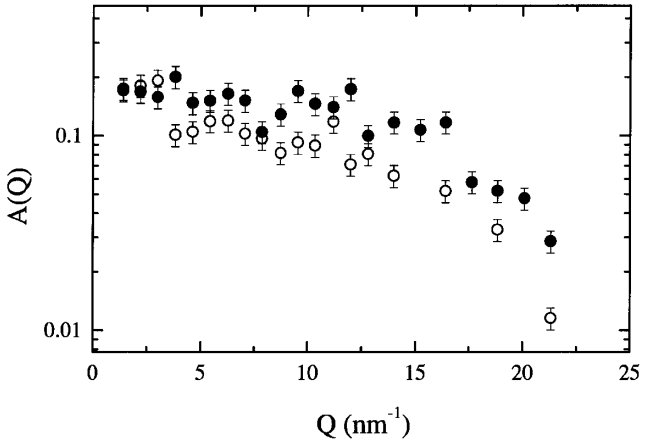

FIG. 2. Ratio, $A(Q)$, of the slow relaxation mechanism strength to the total strength. Full and open circles refer to $T = 475$ and 600 K, respectively.

(resolution-deconvoluted) peak position of the longitudinal current spectrum $\omega^2 S(Q, \omega)$, as obtained by the best-fitted values of the parameters. In the same figure we also report the Q-dependent isothermal sound speed $c_0(Q) = \omega_0(Q)/Q$ (expected to be the limiting value of $c_l(Q)$ at the lowest Q accessible to IXS [12]), as well as

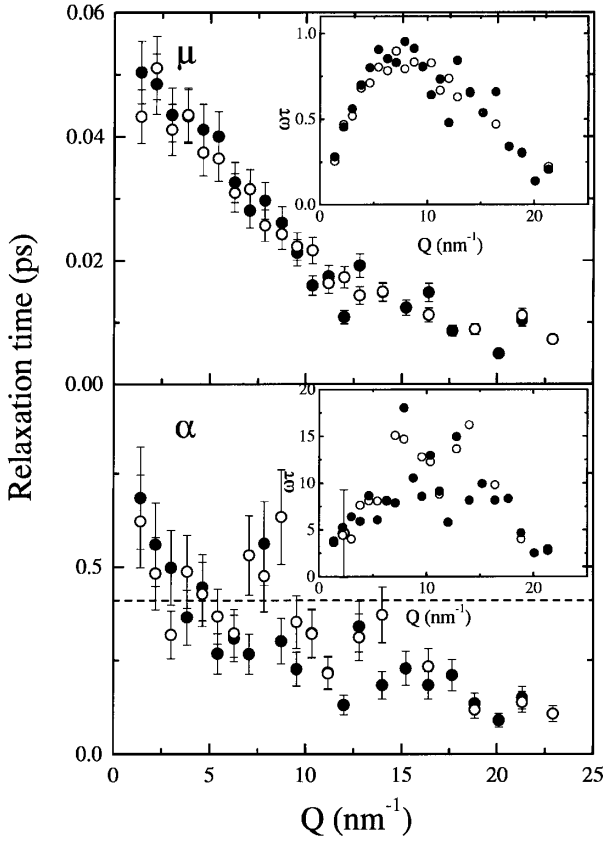

FIG. 3. The times associated with fast (above) and slow (below) relaxation as deduced from the fits. Full and open symbols correspond to $T = 475$ and $T = 600$ K, respectively. A precise determination of the slow structural decay time is affected by the time scale corresponding to the experimental resolution (here 3.3 meV; dashed line).

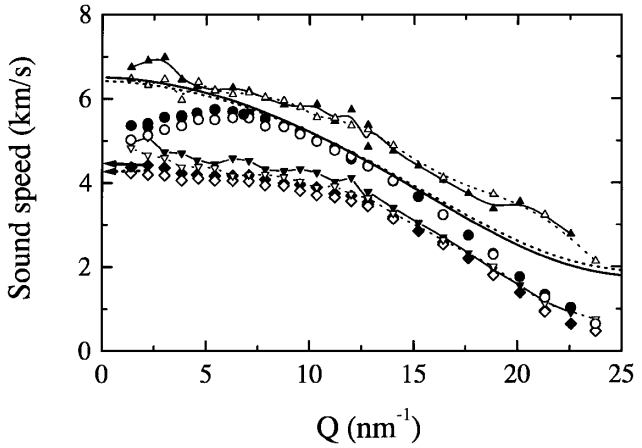

FIG. 4. Effective sound speed $c_l(Q)$ (●) from the peaks of the deconvoluted longitudinal current spectra as deduced from the fits. Also reported are the following: the ordinary hydrodynamic sound speed [17] [arrow (←)], the isothermal speed $c_0(Q)$ (◆), and the instantaneous speed $c_\infty^{\text{th}}(Q)$ (——) as evaluated theoretically in Ref. [12]. Full and open symbols refer to $T = 475$ and 600 K, respectively. From the fitting parameters one may also deduce: (i) $\sqrt{\omega_0^2(Q) + \Delta_\alpha^2(Q)}/Q$ (−▼−), the high-frequency velocity associated with the slow process, and (ii) the total high-frequency velocity $c_\infty(Q)$ (−▲−). The non-coincidence of the latter with the theoretical $c_\infty(Q)$ can be ascribed to the oversimplified form of the memory function model.

the "infinite-frequency" velocity $c_\infty(Q) = [\gamma\omega_0^2(Q) + \Delta_\alpha^2(Q) + \Delta_\mu^2(Q)]^{1/2}/Q$ as obtained from the fit. In principle, the quantity $c_\infty(Q)$ corresponds to an instantaneous, solidlike, response of the liquid and can be evaluated from an integral involving the effective interparticle potential and the pair distribution function [1,12]. To better enlight the different relaxation steps, Fig. 4 also reports the values of $c_{\infty-\alpha}(Q) = [\omega_0^2(Q) + \Delta_\alpha^2(Q)]^{1/2}/Q$, the "unrelaxed" sound speed associated with the presence of the only slow structural mechanism. At the lowest wave vectors probed by IXS, the effective sound velocity $c_l(Q)$ has already reached $c_{\infty\text{-}\alpha}(Q)$; owing to the magnitude of $A(Q)$, its value is, however, only about one-half of the full instantaneous response $c_\infty(Q)$. At larger values of Q it is apparent a "positive dispersion" of $c_l(Q)$, which reaches its maximum at $Q = 6$ nm^{-1}.

At even larger wave vectors ($Q \sim 10$ nm^{-1}), the insets of Fig. 3 show that the condition $\omega_l(Q)\tau_{\alpha,\mu}(Q) \geq 1$ is attained: in this case the effective velocity $c_l(Q)$ is expected to approach the instantaneous value $c_\infty(Q)$. Figure 4 shows that this is indeed the case if $c_\infty(Q)$ is evaluated theoretically from the aforementioned integral. On the other hand, the fact that the values of $c_\infty(Q)$, as calculated from the fit parameters, are larger than the "exact" ones is a consequence of the oversimplified form of the two-exponential decay model in the short-time range relevant for this comparison [12].

Summing up, by IXS it has been possible to detect all the main features of collective dynamics in a simple liquid metal as lithium. Specifically, our data show the presence of three distinct decay channels of the collective memory function. The first one is the "thermal" mechanism: as in other molten alkali metals its relevance is rather small, although not entirely negligible. Much more important is the unambiguous evidence of two well separated time scales in the decay of $M_L(Q,t)$. This provides a convincing experimental demonstration for the simultaneous presence of both fast and slow relaxation processes in the collective dynamics of simple liquids.

[1] U. Balucani and M. Zoppi, *Dynamics of the Liquid State* (Clarendon Press, Oxford, 1994).
[2] A. Rahman, Phys. Rev. A **9**, 1667 (1974); R. D. Mountain, Phys. Rev. A **26**, 2859 (1982); **27**, 2767 (1983); U. Balucani, A. Torcini, and R. Vallauri, Phys. Rev. A **46**, 2159 (1992); S. Kambayashi and G. Kahl, Phys. Rev. A **46**, 3255 (1992); K. Hoshino, H. Ugawa, and M. Watabe, J. Phys. Soc. Jpn. **61**, 2182 (1992); U. Balucani, A. Torcini, and R. Vallauri, Phys. Rev. B **47**, 3011 (1993).
[3] G. Nowotny and G. Kahl, J. Non-Cryst. Solids **205–207**, 855 (1996); U. Balucani, A. Torcini, A. Stangl, and C. Morkel, J. Non-Cryst. Solids **205–207**, 299 (1996).
[4] M. Canales, L. E. Gonzalez, and J. A. Padro, Phys. Rev. E **50**, 3656 (1994); J. Casas, D. J. Gonzalez, and L. E. Gonzalez, Phys. Rev. B **60**, 10 094 (1999).
[5] J. R. D. Copley and J. M. Rowe, Phys. Rev. A **9**, 1656 (1974).
[6] T. Bodensteiner, C. Morkel, W. Glaser, and B. Dorner, Phys. Rev. A **45**, 5709 (1992).
[7] P. Verkerk, P. H. K. deJong, M. Arai, S. M. Bennington, W. S. Howells, and A. D. Taylor, Physica (Amsterdam) **180B–181B**, 834 (1992).
[8] A. Torcini, U. Balucani, P. H. K. deJong, and P. Verkerk, Phys. Rev. E **51**, 3126 (1995).
[9] A. G. Novikov, V. V. Savostin, A. L. Shimkevich, R. M. Yulmetyev, and T. R. Yulmetyev, Physica (Amsterdam) **228B**, 312 (1996).
[10] P. Chieux, J. Dupuy-Philon, J.-F. Jal, and J.-B. Suck, J. Non-Cryst. Solids **205–207**, 370 (1996); D. Pasqualini, R. Vallauri, F. Demmel, C. Morkel, and U. Balucani, J. Non-Cryst. Solids **250–252**, 76 (1999).
[11] H. Sinn *et al.,* Phys. Rev. Lett. **78**, 1715 (1997).
[12] T. Scopigno, U. Balucani, G. Ruocco, and F. Sette, J. Phys. C **12**, 8009 (2000).
[13] An upper estimate of the ratio between the integrated intensity of the one and the two phonon processes (for further details, see, for example, [14]) gives 0.05 at $Q \to 0$. Increasing the wave vector, such contribution further decreases: at $Q = 5$ nm^{-1} it reduces to 0.005.
[14] G. Monaco, A. Cunsolo, G. Ruocco, and F. Sette, Phys. Rev. E **60**, 5505 (1999).
[15] J. P. Boon and S. Yip, *Molecular Hydrodynamics* (McGraw-Hill, New York, 1980).
[16] D. Levesque, J. Verlet, and J. Kurkijarvi, Phys. Rev. A **7**, 1690 (1973).
[17] *Handbook of Thermodynamic and Transport Properties of Alkali Metals,* edited by R. Ohse (Blackwell Scientific, Oxford, 1985).
[18] L. Sjogren, Phys. Rev. A **22**, 2866 (1980); **22**, 2883 (1980).